First publ. in: Biochimica et Biophysica Acta / Molecular basis of disease, 1690 (2004), 1, pp. 22-32

Thermal unfolding of medium-chain acyl-CoA dehydrogenase and iso(3)valeryl-CoA dehydrogenase: study of the effect of genetic defects on enzyme stability

Ibrahim Nasser[a], Al-Walid Mohsen[b], Ilian Jelesarov[c], Jerry Vockley[b,1], Peter Macheroux[d], Sandro Ghisla[a,*]

[a] Department of Biology, University of Konstanz, P.O. Box 5560-M644, D-78457 Konstanz, Germany
[b] Department of Medical Genetics, Mayo Medical School, Rochester, MN 55905, USA
[c] Institute of Biochemistry, University of Zürich, Winterthurerstr. 190, CH-8057 Zürich, Switzerland
[d] School of Engineering and Science, International University Bremen, Campus Ring 6, D-28759 Bremen, Germany

Abstract

Genetic defects affecting acyl-CoA dehydrogenases (ACAD)—key enzymes in the degradation of fatty acids and branched chain amino acids—are increasingly recognized as being more widespread than originally thought. For the medium-chain acyl-CoA dehydrogenase (MCAD), the K304E mutation is the most common genetic defect among Caucasian populations. The effect of substrate or substrate analog binding on the stability of wild-type MCAD and isovaleryl-CoA dehydrogenase (i3VD) and their genetic mutants (K304E- and T168A-MCAD and A282V-i3VD) is examined. Binding to the mutant ACADs is generally ≈ 10-fold weaker compared to wild-type proteins. Thermal stability of wt-MCAD (melting point ≈ 53.6 °C) is significantly higher compared to wt-i3VD (≈ 49.3 °C). With the exception of the A282V-i3VD mutant, a high degree of stabilization (5–11 °C) is induced by conversion into the reduced enzyme form complexed with product. The results are discussed based on the 3D-structures of the enzymes, and it is concluded that in the case of K304E-MCAD thermal stability as such is not a major contribution to the clinical phenotype. With the T168A-MCAD and A282V-i3VD mutants, however, the diminished thermal stability and minor stabilization by ligands must be regarded as an important factor contributing to the manifestation of the disease.

Keywords: Acyl-CoA dehydrogenase; Enzyme stability; Conformational disease

1. Introduction

Acyl-CoA dehydrogenases form a family of FAD-dependent enzymes that currently encompass nine members. They catalyze the same chemical step, the α, β-desaturation of acyl-CoA conjugates, and differ in their specificity for different types of fatty acids linked to CoA [1–3]. Two subfamilies can be differentiated. The first, comprising four members (VLCAD1, ACAD9/VLCAD2, MCAD, and SCAD), acts on ''straight chain'' substrates that are degraded sequentially in the β-oxidation cycle [2]. The second group has five members (LCAD, iBD, i2VD, i3VD, and GD) that are active against branched chain substrates, or the dicarboxylic acid glutarate, degradation product of glutamic acid, in the case of GD [3]. These enzymes and abbreviations derived from their substrate preferences that have been studied recently are listed in Table 1. It should be stated that there can be considerable overlap in the activity profiles and that the mentioned subdivisions can be only orientative.

The best-studied member of the first subfamily is medium-chain acyl-CoA dehydrogenase (MCAD), an enzyme

Abbreviations: 2-aza-iC$_5$-CoA, 2-aza-isovaleryl-CoA[2]

* Corresponding author. Tel.: +49-7531-882291; fax: +49-7531-884161.
E-mail address: Sandro.Ghisla@uni-konstanz.de (S. Ghisla).

[1] Current address: Department of Pediatrics, University of Pittsburgh School of Medicine, Children's Hospital of Pittsburgh, Pittsburgh, PA 15213, USA.

[2] For the abbreviations of enzymes, see Table 1.

Table 1
List of abbreviations of enzymes acting in the α,β-dehydrogenation of fatty acid acyl-CoA conjugates

"Trivial" names of ACADs (alternative names)	Substrate type	Other/alternative abbreviations	Abbreviation
*A*cyl-Co*A* *d*ehydrogenase	Generic		ACAD
*S*hort *c*hain *a*cyl-CoA *d*ehydrogenase (butyryl-CoA dehydrogenase)	Straight	SCADH	SCAD
*M*edium-chain *a*cyl-CoA *d*ehydrogenase	Straight	MCADH	MCAD
*V*ery *l*ong *c*hain *a*cyl-CoA *d*ehydrogenase	Straight	VLCAD, VLCADH	VLCAD1
(Very long chain acyl-CoA dehydrogenase)[a]	Straight/branched (unsaturated)	ACAD-9	VLCAD2[a]
*L*ong *c*hain *a*cyl-CoA *d*ehydrogenase	Straight/branched	LCADH	LCAD
*Iso*butyryl-CoA *d*ehydrogenase	Branched	ACAD-8	iBD
Iso(*3*)*v*aleryl-CoA *d*ehydrogenase	Branched	iVD	i3VD
Iso(*2*)*v*aleryl-CoA *d*ehydrogenase ("short, branched chain" acyl-CoA dehydrogenase), (2-methylbutyryl-CoA dehydrogenase)	Branched	SBCAD, 2mBD ACADSB	i2VD
*G*lutaryl-CoA *d*ehydrogenase	(modified)	GDH	GD

The first five members are thought to be selective for straight chain acyl-CoA substrates, the latter four for branched or modified ones. The newly formulated terms base, respectively, on the differences in activities that have been recognized recently [7].

[a] Unpublished data (Vockley, J. et al.), suggest that this enzyme is active towards substrates with a chain longer than that of VLCAD1 and acts also on unsaturated substrates.

first discovered by Beinert [4]. It has a comparatively broad spectrum of substrate utilization [3], is present at significant quantities in many organs [5], and the three-dimensional structure has been elucidated [6]. This enzyme gained medical relevance upon the discovery, some two decades ago, of an inherited genetic defect, which is among the most frequent ones in humans of northern European descent [2]. A common point mutation causing a K304E replacement is found in 90% of mutant alleles from MCAD deficient patients, and has been associated with heterogeneous clinical symptoms and cellular defects [2,8]. This amino acid is located in the long alpha helix H that forms part of the interface between subunits of the MCAD homotetramer and leads to impaired folding [8,9], low expression of mature protein, instability, and a modified activity spectrum [8].

Another mutation in the MCAD gene in patients with MCAD deficiency leads to an amino acid replacement of threonine 168 to alanine. Threonine 168 is located in the active site of the enzyme in contact with the FAD cofactor and forms a hydrogen bond with the flavin N(5) [10]. The mutant enzyme is stable but only partially active when expressed in heterologous systems. As is seen with the K304E mutation, patients with the T168A mutation present with heterogeneous symptoms [11]. i3VD is the best-studied member of the subfamily involved in the catabolism of amino acids [12]; its biochemical properties have been addressed, and its 3D-structure is known [13]. Several mutations leading to amino acid substitutions have been identified in patients with the clinical disorder isovaleric acidemia (IVA), caused by deficiency of i3VD activity. This disorder can cause a wide spectrum of clinical symptoms, and this may at least in part be related to the level of stability of the mutant enzyme [14]. The most functional i3VD mutants reported are A282V, V342A, and R382L, each of which retains significant partial activity compared to wild-type enzyme when produced in an *E. coli* system. [14].

In a general sense, many of the mutations discovered in patients with enzyme defects in mitochondrial β-oxidation can be classified under the term "conformational diseases," with decreased folding of the mutant protein to a functional form under conditions of physiologic stress [15]. This correlates well with the observation that clinical symptoms in these disorders are often exacerbated by otherwise unrelated underlying illness, especially when associated with fever. In this regard, MCAD and i3VD are appropriate candidates for studying in a semiquantitative manner, the extent to which mutations leading to amino acid substitutions affect protein folding and stability. Study of these processes will provide a better understanding of the effects of physiologic stress on mutant proteins in patients with these disorders, lead to the identification of amino acid motifs and physiologic conditions that help stabilize mutant proteins, and ultimately, the development of therapies designed to improve their stability. In this report, we present thermal stability studies of wild-type, K304E-, and T168A-MCAD enzymes, and wild-type and A282V-i3VD enzymes.

2. Materials and methods

2.1. Materials

Desalting C18 cartridges (Sep-Pak Vac 35 cc C18 cartridges) were from Waters. Hexyl isocyanate from ACROS and isopropyl isocyanate from Aldrich, all other chemicals from Sigma.

2.2. Preparation and purification of acyl-CoA derivatives

Octanoyl-CoA, isovaleryl-CoA, 2-aza-iC_5-CoA, and 2-azaoctanoyl-CoA were synthesized by published procedures [16]. The crude products were desalted using C18

cartridges (30 ml, Waters, elution of salts with H_2O, then of CoAs with 80% methanol). Purity of the products was analyzed by HPLC (Kroma system 2000) using 5 mM potassium phosphate buffer, pH 6.0, (pump A) and a gradient from 5% to 35% MeOH (pump B) over 20 min. The 2-azaoctanoyl-CoA and 2-aza-iC_5-CoA eluted at 16.2 and 11.9 min, respectively. Purities were 94% and 92%, respectively. Concentrations were determined using $\varepsilon_{260} = 20\ mM^{-1}\ cm^{-1}$ for saturated acyl-CoAs [17] and $\varepsilon_{258} = 16\ mM^{-1}\ cm^{-1}$ for 2-aza-acyl-CoAs.

2.3. Purification of enzymes and mutants

wt-MCAD [8], K304E- [8], T168A-MCAD [10], wt-i3VD [14,18], and A282V-i3VD were heterologously expressed in *E. coli* and purified as described in the indicated literature.

2.4. Thermal unfolding

Thermal unfolding of MCAD, i3VD, and their mutants was monitored in 0.1-cm cuvettes using a Jasco J-500 spectropolarimeter at 222 nm. The cuvette was placed in a thermostatted cell holder. The temperature was raised continuously in general from 3 to 93 °C (or as specified) at a heating rate of 1.0 °C/min. In all experiments, the enzyme concentration was ≈ 5 μM in 25 mM potassium phosphate, pH 7.5. Substrate stock solutions were prepared in the same buffer, and added at the indicated final concentration.

2.5. Data analysis

The experimental data ($\theta_{222} = f(T)$) were converted to plots of $F_D = f(T)$ assuming that the ellipticities of the native and denatured state depend linearly on the temperature according to: $\theta_N = \theta_{N,0} + a_N \times T$ (1) and $\theta_D = \theta_{D,0} + a_D \times T$ (2), respectively. $\theta_{N,i}$ and a_i are the coefficients of the linear function describing the pre-transitional and post-transitional portions of the unfolding trace. The fraction of the unfolded protein, F_D, at different temperatures is then given by:

$$F_D = (\theta - \theta_N)/(\theta_U - \theta_N) \quad (3)$$

The melting point, T_m, is the midpoint of transition where $\theta_N = \theta_U = 0.5$. The T_m was calculated from F_U-vs-T curve, where T_m is the temperature at $F_D = 0.5$. The data were processed using the Origin® and KaleidaGraph programs.

3. Results and discussion

3.1. Binding and interactions of ligands and substrates

Acyl-CoA dehydrogenases, and in particular MCAD, for which the data are well documented [19], bind CoA conjugates very tightly, especially those that mimic structural and/or chemical properties of substrate or product [20]. For example: The K_d for binding of enoyl-CoA to reduced wt-MCAD has been estimated to be of the order of 90 nM [21]. Several ACADs are isolated in a green form, where the color is attributed to tightly bound CoA-*S*-persulfide, which remains bound during the purification procedure [22]. Since ligand binding affects stability, and as a basis for understanding the effect of complex formation and change in redox state on thermal unfolding and stability, we have addressed these topics in some detail. It is important to note that the interaction of ligands and substrates with ACADs is a complex process [3], the salient components of which are shown in Scheme 1. The complexation is relatively tight with a $K_d \approx 5$ μM, as is derived from plots of the absorbance changes at the maxima of the difference spectra (Fig. 1, insert A). While the pattern of the difference spectra (Fig. 1, insert B) is overall similar to that reported by Thorpe's group for MCAD [17], there is a substantial difference: With i3VD there is a weak,

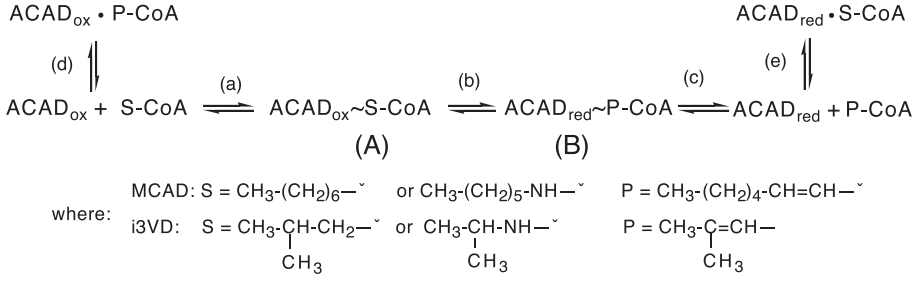

Scheme 1. Equilibria present in a system containing ACADs and substrates (adapted from Refs. [3,25]. Step (a) is binding of ligand/substrate (S-CoA), and probably consists of several steps involving not shown intermediates that lead to complex (A). In the case of substrate step (b) follows, which reflects the chemical oxidoreduction equilibrium linking (A) to (B), the complex of reduced enzyme with enoyl-CoA product (ACAD$_{red}$ ~ P-CoA). This probably consists of two species in rapid equilibrium (not shown) and is characterized by a green to blue color arising from a charge transfer interaction. Dissociation of product (P-CoA) from (B) (step c) is thermodynamically very unfavorable (K_ds < 0.1 μM), relatively slow [21], and leads to free P-CoA and free reduced enzyme ACAD$_{red}$. The latter, in turn, can bind excess substrate (step e), while free product (P-CoA) can bind to free oxidized ACAD (step d). The reaction of substrate with ACAD will thus lead to a mixture of species that are linked by rapid or slow equilibria, and wherein the relative concentrations of the components will depend on temperature, on the concentrations of S-CoA and P-CoA, and on specific equilibrium constants. In the second type of species, 2-aza-CoA substrate analogs, an amidic NH replaces a CH_2 at position α and mimics substrate in forming complex (A). However, due to the chemical modification, they do not react to (B).

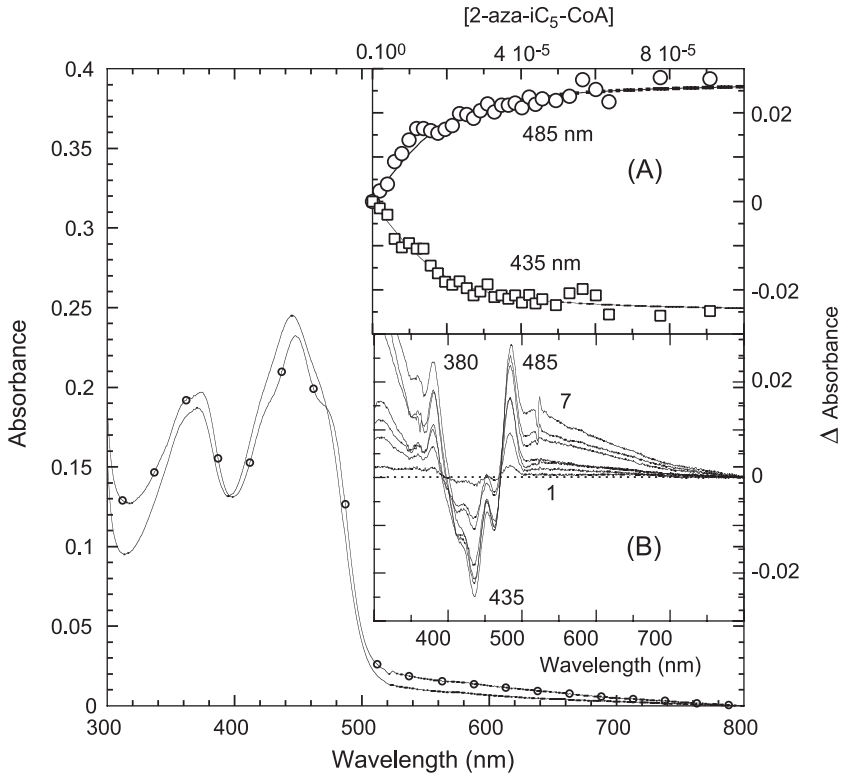

Fig. 1. Binding of the substrate analog 2-aza-iC$_5$-CoA to wild-type i3VD. (Curve —) is the absorption spectrum of free enzyme, 18 μM in 50 mM Tris−Cl buffer, pH 8.0 and at 25 °C. Curve (−○−) was obtained upon addition of a total of 72 μM of the ligand (corrected for dilution). Insert (B) shows selected difference spectra obtained upon addition of (1) 2, 6, 16, 20, 46, 60 and (7) 96 μM of the ligand. Insert (A) depicts the changes at the indicated wavelengths as a function of added ligand. The lines are the fits obtained with the mass equation.

but significant absorbance extending from 500 to 800 nm observable both in the main panel and in the difference spectra which has a maximum around 510 nm (Fig. 1, panel B). This is attributed to a charge transfer transition that is typical for ACAD complexes involving a negatively charged or electron-rich ligand and oxidized flavin cofactor [3]. However, 2-aza-iC$_5$-CoA as such is not a donor; it becomes one upon deprotonation of the 2-aza-function.

There are several examples of analogs that become deprotonated at the α-position upon binding to MCAD, two prominent ones being acetoacetyl-CoA and 3S-C$_8$-CoA [23,24]. The fact that the charge transfer intensity is weak could be due to a low intrinsic extinction coefficient. However, it is more probable that under the specific conditions of Fig. 1, the equilibrium (pK) of Scheme 2. The perturbation of the oxidized flavin spectrum is comparable to that observed with wt-i3VD (compare difference spectra

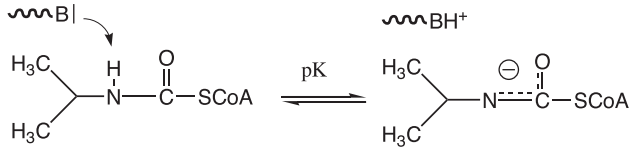

Scheme 2. Mode of deprotonation of the 2-aza-iC$_5$-CoA analog at the active site of i3VD.

in Figs. 1 and 2) suggesting that the binding modus is the same. However, the binding constant K_d is one order of magnitude higher. This can be attributed to the larger volume of the valine isopropyl side chain compared to the methyl of alanine. This volume increase would not allow as tight a "closing" of the substrate binding cleft compared to wt-i3VD.

Addition of substrate to ACADs leads to the setup of the equilibria depicted in the Scheme 1 [3,25]. While the true situation is more complex [21], this minimal scheme should be adequate for the present case. The apparent binding constant $K_{d,app}$ deduced from the dependence of spectral effects on the amount of added substrate will thus reflect all involved steps, and in particular step (b), the internal redox equilibrium of the system. In the case of wild-type MCAD, $K_{d,app}$ for the best substrate octanoyl-CoA can be estimated as around 0.1−1 μM [21], and the prevalent species formed with a small excesses of octanoyl-CoA is reduced enzyme [26]. $K_{d,app}$ is somewhat weaker for the K304E and T168A mutants (Table 2) as can be deduced from the extent of reduction of the oxidized enzymes [8,10].

The behavior observed with i3VD is qualitatively similar. Addition of isovaleryl-CoA to i3VD leads to essentially complete reduction of the oxidized enzyme flavin with a $K_{d,app} \leq 1$ μM (Mohsen, A.W., and Vockley, J., in preparation). This interaction is severely affected by the

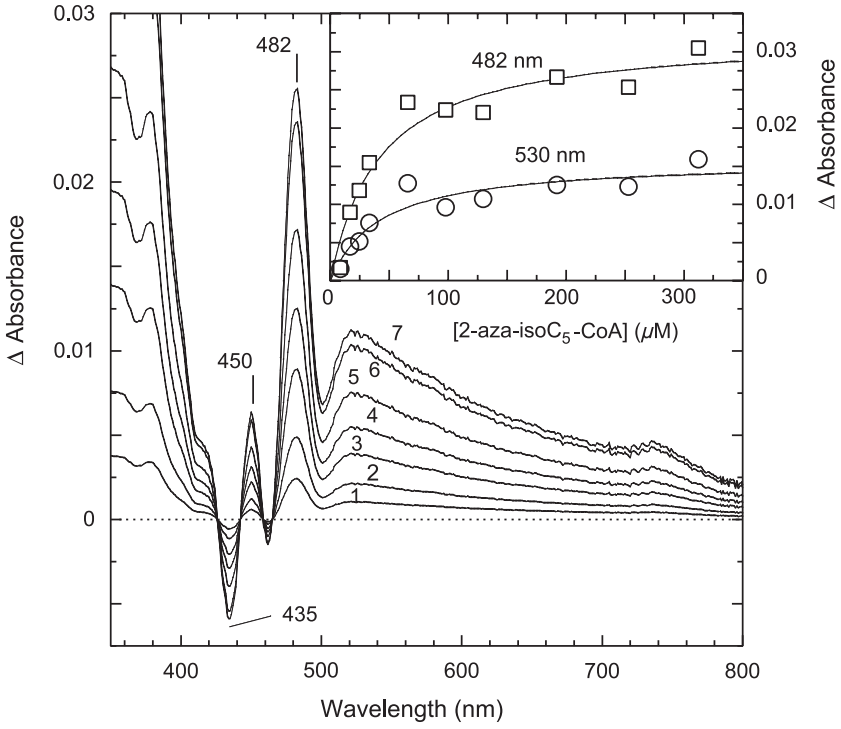

Fig. 2. Interaction of A282V-i3VD with the substrate analogue 2-aza-iC$_5$-CoA. General conditions as detailed in the legend of Fig. 1. Increasing amounts of the ligand were added to the enzyme, the starting spectrum of which corresponds to Curve (1) in Fig. 3. The main panel depicts the difference spectra obtained from subtraction of the initial spectrum from that at the given titration point. Only selected spectra are shown that correspond to addition of (1) = 8, (2) = 17, (3) = 25, (4) = 33, (5) = 98, (6) 192, and (7) = 312 μM ligand (see insert for further titration points). All spectra and data points are corrected for dilution. Analysis of the primary data was done with the global fitting program "Specfit-32" (that employs data points at all wavelengths) and the traces in the main panel were obtained by a smoothing procedure of this program. The global procedure yields an apparent $K_d = 36 \pm 8$ μM. The analysis in the insert is for the two specific wavelengths shown and yields apparent K_ds = 41 ± 9 (482 nm) and = 42 ± 13 μM (530 nm).

A282V mutation, where, in comparison to wt-i3VD, the $K_{d,app}$ of the mutant for the substrate is approximately two orders of magnitude higher and reduction occurs only to ≈ 60%. The latter can be deduced from the extent of absorbance decrease in the 450 nm area that is due to disappearance of the band of the oxidized flavin chromophore (Fig. 3), and in comparison to wt-i3VD, where upon incubation with excess substrate iC$_5$-CoA removal of the oxidized flavin absorbance is essentially complete (Mohsen, A.W., and Vockley, J., in preparation). This behavior is consistent with that found for the overall reaction using the ETF reduction assay [14]. It implies that the substrate binding step (Scheme 1, a) is also impaired as with the 2-aza-analog, and that the internal redox equilibrium (Scheme 1, b) is not shifted completely to the right as with wt-i3VD.

3.2. Thermal unfolding of wild-type MCAD and wild-type i3VD

Thermal unfolding of wt-MCAD was measured as a function of temperature from 4 to 75 °C as shown in Fig. 4. The data show that denaturation of wt-MCAD depends on its state of oxidation and on the presence of ligand. The melting transition of the unliganded, oxidized wt-MCAD enzyme is broad, extending from ~ 42 to ~ 60 °C and displaying a shoulder on the low-temperature side (Fig. 4, insert). Differently, melting is much more sharp and symmetric in the presence of ligands. This suggests most likely that the unliganded protein denatures through an intermediate. Addition of ligands apparently stabilizes the enzyme and increases the cooperativity of thermal melting.

This behavior does not appear to apply for i3VD (Fig. 5), since the first derivative profiles are comparatively sharp and symmetric. Comparison of the data for the two enzymes (Table 1) indicates that MCAD denatures at significantly higher temperature than i3VD.

As discussed above, substrate leads to reduction of ACADs and this is reflected by a stabilization corresponding to an increase of the melting point by 6 (i3VD) up to 10 °C (MCAD) (Table 2, Fig. 5). In the presence of the substrate analog 2-aza-octanoyl-CoA that forms complex (A) (Scheme 1) there is an increase by ≈ 1–4 °C. The differences in melting temperatures induced by the two types of CoA (substrate vs substrate analog) thus reflect the differences in interaction, respectively, with oxidized and reduced MCAD, and indicate that the factors involving the redox process are quantitatively more important than the binding process for thermal stability.

Interestingly, with wt-MCAD the reaction with substrate and 2-aza-ligand leads to a much sharper transition (Fig. 2,

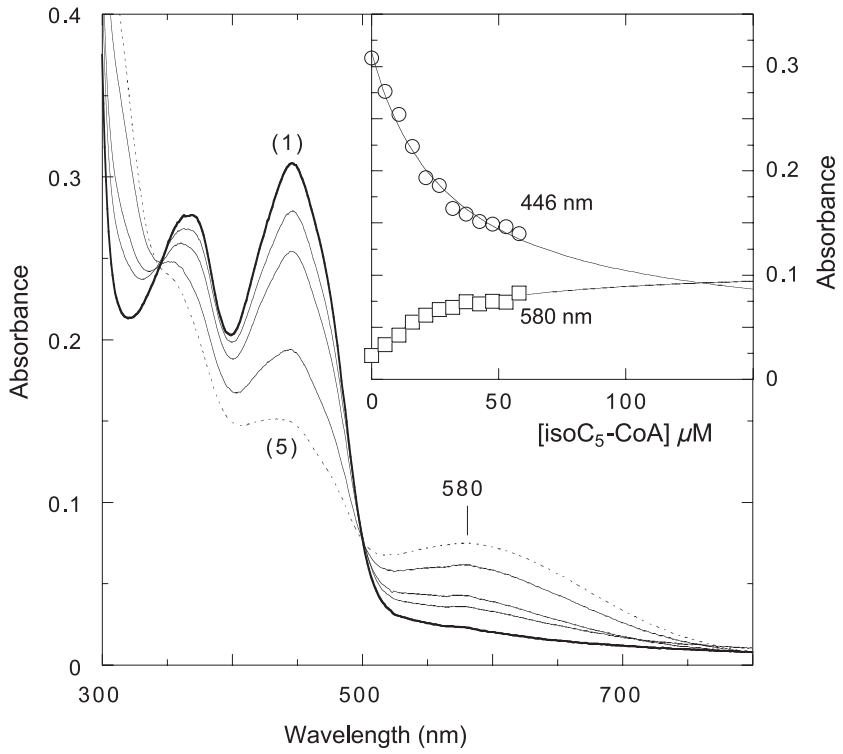

Fig. 3. Interaction of A282V-i3VD with the substrate isovaleryl-CoA. The main panel depicts the spectral course of the anaerobic titration of the enzyme, ≈ 20 μM in 50 mM Tris–HCl, pH 8.0 and at 25 °C with increasing aliquots of isovaleryl-CoA. Curve (1) is the spectrum of free enzyme, next curves to (5) are the species that were obtained in the presence of ≈ 5, 11, 21, 60 μM substrate. The inset shows the dependence of the spectral changes from the indicated concentrations of added substrate recorded at wavelengths where they are maximal. The full lines are the fits obtained using the mass law equation and yield "interaction constants" (apparent K_ds) of 30 ± 6 μM (446 nm) and 26 ± 6 μM (580 nm). The spectra and data points are corrected for dilution. See text for further details.

insert) compared to unliganded enzyme. Thus, free MCAD might exist in several conformers having marginally different melting temperatures and is converted upon ligand binding into single species corresponding to (A) or (B), respectively; Scheme 1. Comparison of the same phenomena for MCAD and i3VD uncovers greater stabilization by substrate for MCAD compared to i3VD (7–10 vs ≈ 6 °C, Table 2).

3.3. Effect of genetic mutations on thermal stability

In previous experiments the activity of the K304E and T168A mutants were compared to that of wt-MCAD by assessing the activity upon a definite time of incubation at different temperatures [8,10]. It was estimated that the activity decreases to 50% of the maximal value at ≈ 52 and ≈ 41 °C for the K304E and T168A-MCAD mutants, respectively. The latter was completely inactivated after 20-min incubation at 41 °C [10]. However, this type of experiments does not take into account the effect of ligands/substrate and constitutes only a rather crude estimate. This is of importance since ligation and the redox state have pronounced effects on the stability of ACADs [27]. We have examined this directly with thermal denaturation experiments (Fig. 6).

The K304E-MCAD mutant was found to unfold at ≈ 3.5 °C lower than wt-enzyme. However, the K304E mutant protein responds to the presence/addition of the substrate octanoyl-CoA in a very similar way, the stabilizing effect is thus similar for both proteins (Table 2) consistent with an analogous thermodynamic effect accompanying formation of reduced enzyme. From this it can be concluded that, under physiological conditions, thermal instability is not a major factor responsible for the observed clinical effects. Previous studies had concluded that the mutation mainly affected the "conformation" of the K304E-MCAD protein [28] in addition to its capacity to be expressed in a soluble, active form [29], and to effects on its catalytic properties/specificity [8]. The data presented here clearly support the importance of these factors. In contrast to the K304E mutant, the T168A-MCAD variant has a greatly reduced thermal stability both as a free protein, as well as in the presence of a substrate or substrate analog (Table 2). The extent of thermal destabilization induced by the T to A replacement suggests that it is a (major) source for protein instability in vivo and hence a molecular cause for the observed clinical symptoms.

3.4. Comparison of the data with structural information

The present results provide a semiquantitative picture of the factors that affect unfolding of two of the best-studied members of the ACAD family, MCAD and i3VD. They also

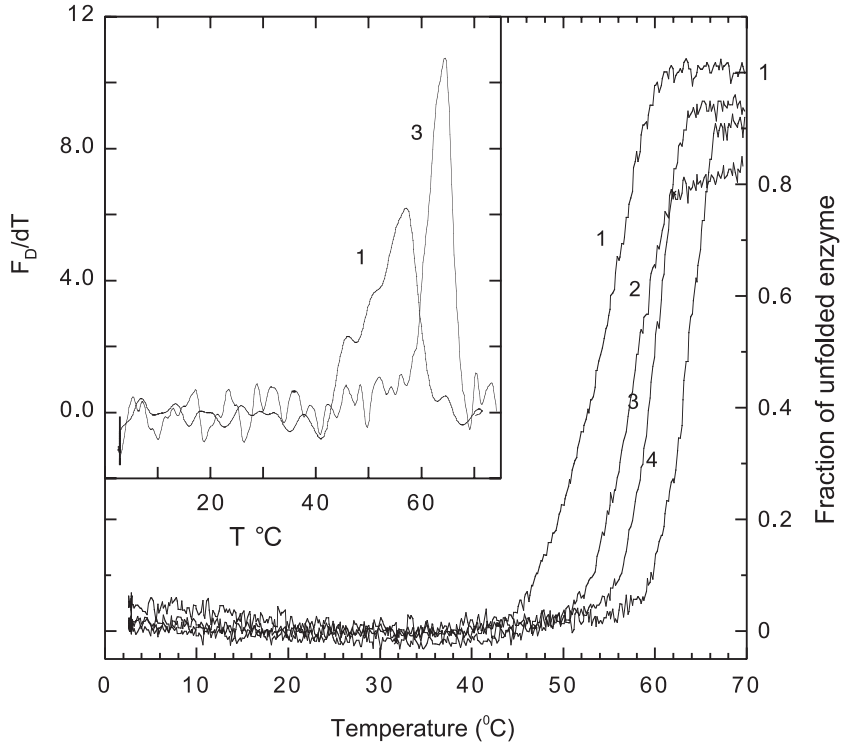

Fig. 4. Thermal unfolding curves of wt-MCAD. Main panel: (1) in the absence of substrate; (2) in the presence of 20 μM 2-aza-C_8CoA; (3 and 4) in the presence of 20 and 300 μM C_8CoA. The spectra were normalized for the values of intact proteins and changes were followed by far-UV CD at λ_{222} nm. Conditions are detailed in Materials and methods. Insert: First derivative of the CD spectra for curves (1) and (3).

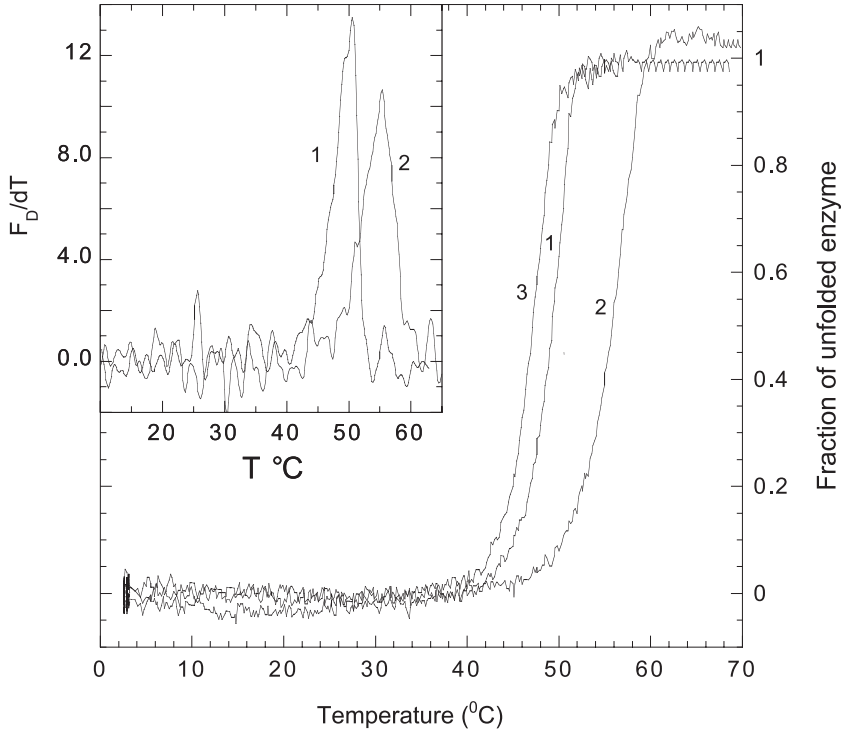

Fig. 5. Thermal unfolding curves of wt-i3VD. Main panel: (1) in the absence of substrate, (2) in the presence of 20 μM iC_5CoA, and (3) in the presence of 20 μM 2-aza-iC_5CoA. Normalization and conditions as in Fig. 4. Insert: First derivative of the CD spectra for curves (1) and (2).

Table 2
Apparent melting points of MCAD, i3VD and of mutants and effect of substrate or ligand binding

	Enzyme, form	Substrate/ligand		T_m/°C	Substrate/ligand (apparent) K_d
		Structure	Concentration/μM		
MCAD	Wild-type, ox	None		56.4	–
	ox/red	C_8-CoA,	20	63.5	0.1–1 μM [17]
	red	C_8-CoA,	300	66.9	
	ox	2-aza-C_8-CoA	20	59.3	0.05 μM [17]
	K304E, ox	None		53	–
	ox/red	C_8-CoA	20	60	≥ 1 μM (a)
	red	C_8-CoA	300	64	
	ox	2-aza-C_8-CoA	20	59.1	≈ 0.5 μM
	T168A, ox	None		46.7	–
	ox/red	C_8-CoA	20	52.5	≥ 1 μM (a)
	red	C_8-CoA	300	58.1	
	ox	2-aza-C_8-CoA	20	52.1	nd
i3VD	Wild-type, ox	None		50.5	–
	ox/red	iV-CoA	20	55.4	= 1 μM (b)
	ox	2-aza-iC_5-CoA	20	50.9	≈ 5 μM
	A282V, ox	None		48.2	–
	ox/red	iV-CoA	20	48.5	≈ 30 μM
	ox	2-aza-iC_5-CoA	20	48.6	≈ 40 μM

The abbreviations ox, red and ox/red stand for oxidized, reduced, or a mixture of these species; iV = isovaleryl. (a) As explained in the text this value is a rough estimate that reflects the equilibrium situation described by Scheme 1. (b) Mohsen, W. and Vockley, J., unpublished data.

deepen and partially modify our understanding of the effects of genetically determined mutations affecting ACADs. Comparison of the melting temperatures for the various forms of MCAD and i3VD (Table 2, Figs. 4–6) suggests that the thermal stability of wild-type MCAD is rather high compared to that of i3VD; a difference of 6 °C in the melting temperature is significant. The overall supersecondary or quaternary structures of the two enzymes are very similar, with the exception of a disulfide bond between Cys318 and Cys323 in the loop connecting α-helices H and I present in i3VD [13]. A specific reason for this difference is thus not evident. On the other hand, it should be kept in mind that FAD binding/affinity is important in protein stability [30]. While there are no quantitative data on the

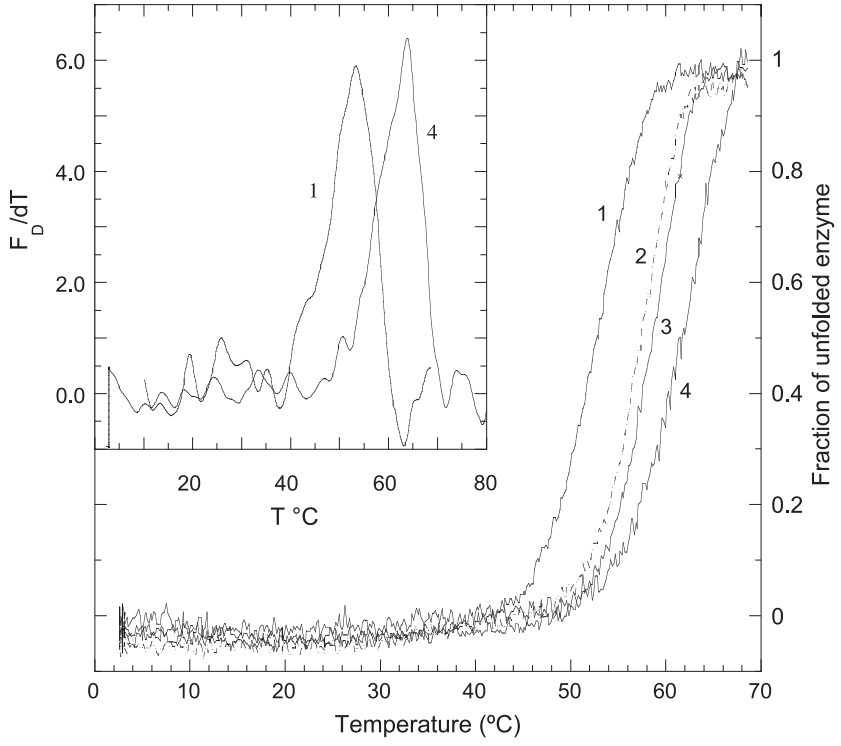

Fig. 6. Thermal unfolding curves of K304E-MCAD. Main panel: (1) in the absence of substrate; (2) in the presence of 20 μM 2-aza-C_8CoA; (3 and 4) in the presence of 20 and 300 μM C_8CoA. Normalization and conditions as in Fig. 4. Insert: First derivative of the normalized CD spectra for curves (1) and (3).

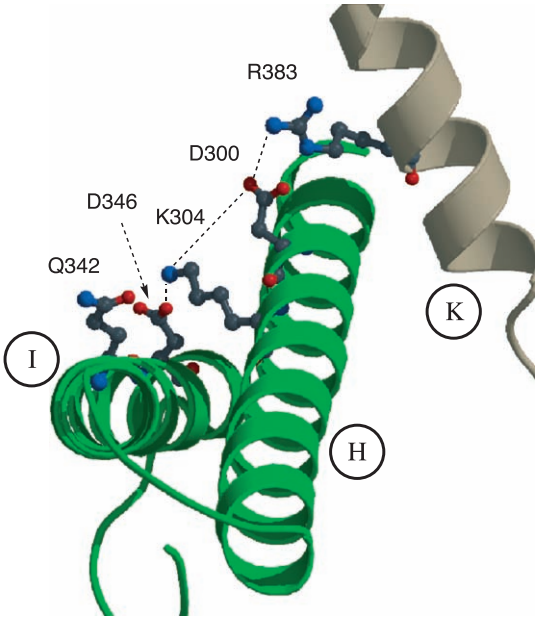

Fig. 7. Three-dimensional representation of the location of the K304E-mutation in MCAD. Helices (I), (H) belong to a different subunit than (K). They are part of the interface domain of homotetrameric MCAD. It should be noted that the K304E-mutation will affect the balance of charges of the D346, K304, D300 and R383 groups and consequently is likely to influence their reciprocal positioning/orientation.

affinity of MCAD for FAD compared to i3VD, unpublished evidence suggests that FAD affinity is lower in the case of i3VD. As an example, T168-OH forms a tight H-bond to the flavin N-5 position both in MCAD and i3VD [6]; its removal as with the T168A-MCAD mutant greatly reduces the affinity for FAD [10]. While the T168A-MCAD mutant is produced in *E. coli*, and can be purified, if FAD is present in buffers during purification, this is not the case with the corresponding T168A-i3VD mutant (Mohsen, A.W. and Vockley, J., unpublished). This is consistent with a significantly weaker FAD binding of wt-i3VD that translates into a lower stability, and with a further weakening in the case of the A282V-i3VD mutant. In a general sense, it appears that thermal stability is substantially lower in i3VDs compared to MCAD, the same holding for the corresponding mutants (Table 2).

The −OH group of T168 in MCAD is positioned exactly in the projection of the flavin plane, and forms a tight H-bond (2.9 Å) with the flavin N(5), the entry point for hydride during catalysis. An identical situation is found in i3VD [13]. A specific role for such an H-bond also is probable since the activity of the mutant is substantially reduced [10]. It is known [24] that for wt-MCAD the pK for the abstraction of a CoA ligand αC-H is lowered by ≥ 10 pK units at the active center. With T168A-MCAD the pK shift is much smaller (≤ 5 pK units, R. Gradinaru and S. Ghisla, unpublished data) corresponding to a difference of ≈ 7 kcal/mol. This is corroborated by the observation of a similar effect with wt-MCAD in which the native FAD cofactor has been replaced by its 5-deaza-FAD analog (Gradinaru and S. Ghisla, unpublished data). Deaza flavins cannot form such H-bonds. In addition, the Thr168-OH might also serve in the fixation/positioning of the flavin [6,10] and thus indirectly affect the stability of the protein [30]. In the context of enzyme stability, it thus appears that this simple H-bond might be unusually important as reflected by the large effect on enzyme thermal unfolding. Along this line of reasoning, it can be deduced that the substantially modified activity vs. chain length profile exhibited by T168A-MCAD compared to wt enzyme [10] is due to enhanced flexibility at the active center.

The effect of genetic mutations on protein melting points is best represented by the K304E-MCAD case. Previous studies had concluded that the mutation mainly affected the "conformation" of the enzyme [28] in addition to its capacity to be expressed in a soluble, active form [29], and to effects on its catalytic properties and the chain length specificity [8]. While the melting behavior confirms the diminished stability of this protein, the observed effect is comparatively small. Interestingly, substrate binding restores the thermal stability of the K304E mutant protein approximately to the level of wild-type enzyme. Inspection of the dimer–dimer interface domain of MCAD that is part of the homotetrameric native structure (Fig. 7) shows that K304 is part of a quaternary interaction of the groups R383, D300, K304 and D346 located on helices J, H and K (Fig. 7). Hence, it is probable that a K304E mutation affects the strength of the salt bridge between D300 and R383 (Fig. 7) and that this, in turn, affects the tertiary/quaternary structure.

Turning to i3VD, the lack of substantial changes in the melting temperature of the genetic A282V mutant in the

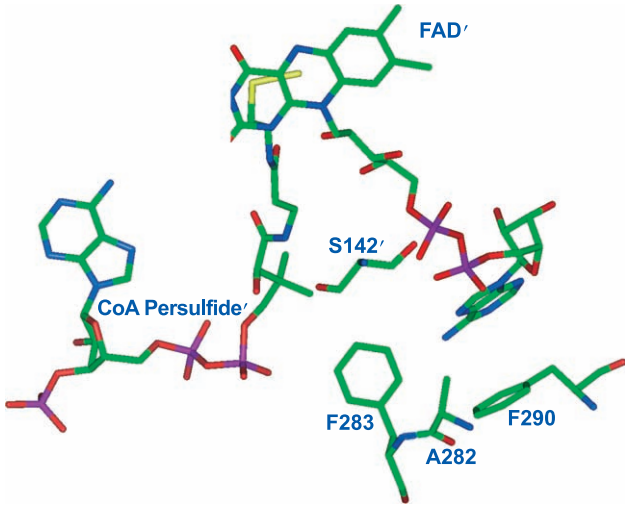

Fig. 8. Position of A282 in i3VD relative to the cofactor FAD. This group is located near the interface of two subunits of the homotetrameric enzyme and in close proximity to the adenylate moiety of FAD. In the A282V mutant the larger size of the valine side chain is likely to "force open" the cleft serving for the binding of the FAD AMP moiety. (The prime sign denotes ligand or residue of the second subunit). Adapted from Ref. [13].

presence of ligand and substrate, and as compared to wt-i3VD, is relevant. This is consistent with the mutant having substantially weaker affinities for ligands (Table 2) and also a ≈ 35-fold lower activity [14]. Also in this case the A282V mutation is considerably distant from the active centers, of the same subunit (≈ 41 Å) or the neighboring subunit (≈ 17 Å). It is, however, in close proximity to residues constituting the FAD′ adenine binding cleft (the prime sign denotes ligand or residue of the second subunit). Fig. 8 shows that it is located at the monomer–monomer interface near the amino acid side chains of F290 that are in contact with the adenosyl moiety of FAD. In addition, F283, which would be above the plane of the figure, is 3.5 Å away from the C_β of the A282 and 3.2 Å away from the FAD′ adenine, apparently providing π–π interaction to the latter.

Examination of the arrangements in Fig. 8 suggests that replacement of alanine with a valine would affect binding of FAD by disrupting the interactions of its AMP moiety with the above residues. This, in turn, might affect the interactions of S142′ with the adenosyl moiety of FAD and the pantetheine moiety of the CoA ligand and consequently impair binding of the latter. Another possible effect for the A282V replacement is that the valine side chain in the mutant would force the side chain of F283, which is 4 Å away from the phosphate of the AMP′ moiety of the i3V-CoA′ in the published model [13], to adopt a slightly different conformation bringing it closer to this possibly charged phosphate and hence disrupting substrate binding.

It has been difficult to show genotype/phenotype correlations for mutations identified in patients with MCAD deficiency. Heterogeneous symptoms have been reported in patients with the common K304E mutation as well as in others seen in more than one patient. The present data substantiate the assumption that with this mutant thermal instability as such is not a major factor in disease manifestation, as opposed to the effects on efficiency of de novo folding. With the T168A mutation, however, thermal instability of the already processed and folded protein is much more pronounced arguing that it is a major molecular cause for the observed symptoms. Patients having i3VD mutations that lead to an enzyme with partially reduced activity and/or stability tend to have milder clinical symptoms than those with mutations leading to lack of enzyme protein at the cellular level. In such cases, reduced thermal stability of a mutant enzyme may play a role in the development of symptoms during times of illness, especially those associated with fever. Study of additional patients and mutations will be necessary to substantiate this.

Acknowledgements

This work was supported in part by grants from the Deutsche Forschungsgemeinschaft (Gh 2/6-4) to S.G, and by PHS grant RO1 DK45482 to J.V.

References

[1] J.J. Kim, R. Miura, Acyl-CoA dehydrogenases and acyl-CoA oxidases. Structural basis for mechanistic similarities and differences, Eur. J. Biochem. 271 (2004) 483–493.
[2] N. Gregersen, P. Bross, B.S. Andresen, Genetic defects in fatty acid beta-oxidation and acyl-CoA dehydrogenases, Molecular pathogenesis and genotype–phenotype relationships, Eur. J.Biochem. 271 (2004) 470–482.
[3] S. Ghisla, C. Thorpe, Acyl-CoA Dehydrogenases: a mechanistic overview, Eur. J. Biochem.,(in press).
[4] H. Beinert, , 2nd ed., P.D. Boyer, H. Lardy, K. Myrback (Eds.), The Enzymes vol. 7,Academic Press, New York, 1963, pp. 447–466.
[5] M. Nagao, B. Parimoo, K. Tanaka, Developmental, nutritional, and hormonal regulation of tissue-specific expression of the genes encoding various acyl-CoA dehydrogenases and alpha-subunit of electron transfer flavoprotein in rat, J. Biol. Chem. 268 (1993) 24114–24124.
[6] J.J. Kim, M. Wang, R. Paschke, Crystal structures of medium-chain acyl-CoA dehydrogenase from pig liver mitochondria with and without substrate, Source (Bibliographic Citation), Proc. Natl. Acad. Sci. U. S. A. 90 (1993) 7523–7527.
[7] M. He, T.P. Burghardt, J. Vockley, A novel approach to the characterization of substrate specificity in short/branched chain Acyl-CoA dehydrogenase, J. Biol. Chem. 278 (2003) 37974–37986.
[8] V. Kieweg, F.G. Krautle, A. Nandy, S. Engst, P. Vock, A.G. Abdel-Ghany, P. Bross, N. Gregersen, I. Rasched, A. Strauss, S. Ghisla, Biochemical characterization of purified, human recombinant Lys304→Glu medium-chain acyl-CoA dehydrogenase containing the common disease-causing mutation and comparison with the normal enzyme, Eur. J. Biochem. 246 (1997) 548–556.
[9] T. Saijo, W.J. Welch, K. Tanaka, Intramitochondrial Folding and Assembly of Medium-Chain Acyl-CoA Dehydrogenase (MCAD)—Demonstration of Impaired Transfer of K304E-Variant MCAD from Its Complex with Hsp60 to the Native Tetramer, J. Biol. Chem. 269 (1994) 4401–4408.
[10] B. Kuchler, A.G. Abdel-Ghany, P. Bross, A. Nandy, I. Rasched, S. Ghisla, Biochemical characterization of a variant human medium-chain acyl-CoA dehydrogenase with a disease-associated mutation localized in the active site, Biochem. J. 337 (1999) 225–230.
[11] B.S. Andresen, P. Bross, S. Udvari, J. Kirk, G. Gray, S. Kmoch, N. Knudsen, I. Knudsen, V. Winter, B. Wilcken, I. Yokota, K. Hart, S. Packman, J.P. Harpey, J.M. Saudubray, D.E. Hale, L. Bolund, S. Gregersen, N. Gregersen, The molecular basis of medium-chain acyl-CoA dehydrogenase (MCAD) deficiency in compound heterozygous patients: is there correlation between genotype and phenotype?, Hum. Mol. Genet. 6 (1997) 695–707.
[12] Y. Ikeda, K. Tanaka, Purification and characterization of isovaleryl coenzyme A dehydrogenase from rat liver mitochondria, J. Biol. Chem. 258 (1982) 1077–1085.
[13] K.A. Tiffany, D.L. Roberts, M. Wang, R. Paschke, A.W. Mohsen, J. Kim, J.J. Kim, Structure of human isovaleryl-CoA dehydrogenase at 2.6 A resolution: structural basis for substrate specificity, Biochemistry 36 (1997) 8455–8464.
[14] A.W. Mohsen, B.D. Anderson, S.L. Volchenboum, K.P. Battaile, K. Tiffany, D. Roberts, J.J. Kim, J. Vockley, Characterization of molecular defects in isovaleryl-CoA dehydrogenase in patients with isovaleric acidemia, Biochemistry 37 (1998) 10325–10335.
[15] P. Bross, T.J. Corydon, B.S. Andresen, M.M. Jorgensen, L. Bolund, N. Gregersen, Protein misfolding and degradation in genetic diseases, Human Mutat. 14 (1999) 186–198.
[16] W. Seubert, S-Palmytoyl CoA, Biochem. Prep. 7 (1960) 80–83.
[17] R.C. Trievel, R. Wang, V.E. Anderson, C. Thorpe, Role of the carbonyl group in thioester chain length recognition by the medium chain acyl-CoA dehydrogenase, Biochemistry 34 (1995) 8597–8605.

[18] A.W. Mohsen, J. Vockley, High-level expression of an altered cDNA encoding human isovaleryl-CoA dehydrogenase in *Escherichia coli*, Gene 160 (1995) 263–267.
[19] P.J. Powell, S.M. Lau, D. Killian, C. Thorpe, Interaction of acyl coenzyme A substrates and analogues with pig kidney medium-chain acyl-coA dehydrogenase, Biochemistry 26 (1987) 3704–3710.
[20] P.J. Powell, S.-M. Lau, C. Thorpe, Interaction of acyl-CoA substrates and analogues with pig kidney medium chain acyl-CoA dehydrogenase, Biochemistry 26 (1987) 3704–3710.
[21] J.G. Cummings, S.M. Lau, P.J. Powell, C. Thorpe, Reductive half-reaction in medium-chain acyl-CoA dehydrogenase: modulation of internal equilibrium by carboxymethylation of a specific methionine residue, Biochemistry 31 (1992) 8523–8529.
[22] G. Williamson, P.C. Engel, J.P. Mizzer, C. Thorpe, V. Massey, Evidence that the greening ligand in native butyryl-CoA dehydrogenase is a CoA persulfide, J. Biol. Chem. 257 (1982) 4314–4320.
[23] I. Rudik, C. Thorpe, Thioester enolate stabilization in the acyl-CoA dehydrogenases: the effect of 5-deaza-flavin substitution, Arch. Biochem. Biophys. 392 (2001) 341–348.
[24] P. Vock, S. Engst, M. Eder, S. Ghisla, Substrate activation by acyl-CoA dehydrogenases: transition-state stabilization and pKs of involved functional groups, Biochemistry 37 (1998) 1848–1860.
[25] L.M. Schopfer, V. Massey, S. Ghisla, C. Thorpe, Oxidation-reduction of general acyl-CoA dehydrogenase by the butyryl-CoA/crotonyl-CoA couple. A new investigation of the rapid reaction kinetics, Biochemistry 27 (1988) 6599–6611.
[26] C. Thorpe, R.G. Matthews , C.H. Williams Jr., Acyl-coenzyme A dehydrogenase from pig kidney. Purification and properties, Biochemistry 18 (1979) 331–337.
[27] M. Madden, S.M. Lau, C. Thorpe, The influence of oxidation-reduction state on the kinetic stability of pig kidney general acyl-CoA dehydrogenase and other flavoproteins, Biochem. J. 224 (1984) 577–580.
[28] P. Bross, T.J. Corydon, B.S. Andresen, M.M. Jorgensen, L. Bolund, N. Gregersen, Protein misfolding and degradation in genetic diseases, (Review)Human Mutat. 14 (1999) 186–198.
[29] P. Bross, B.S. Andresen, V. Winter, F. Krautle, T.G. Jensen, A. Nandy, S. Kolvraa, S. Ghisla, L. Bolund, N. Gregersen, Co-overexpression of bacterial GroESL chaperonins partly overcomes non-productive folding and tetramer assembly of *E. coli*-expressed human medium-chain acyl-CoA dehydrogenase (MCAD) carrying the prevalent disease-causing K304E mutation, Biochim. Biophys. Acta 1182 (1993) 264–274.
[30] T. Saijo, J.J. Kim, Y. Kuroda, K. Tanaka, The roles of threonine-136 and glutamate-137 of human medium chain acyl-CoA dehydrogenase in FAD binding and peptide folding using site-directed mutagenesis: creation of an FAD-dependent mutant, T136D, Arch. Biochem. Biophys. 358 (1998) 49–57.